



OPEN

SUBJECT AREAS:

CHEMISTRY

PHYSICAL CHEMISTRY

SPECTROSCOPY

FLUORESCENCE SPECTROMETRY

Photoluminescence from Amino-Containing Polymer in the Presence of CO₂: Carbamato Anion Formed as a Fluorophore

Xiaoyong Pan¹, Guan Wang¹, Chee Leng Lay¹, Beng Hong Tan¹, Chaobin He^{1,2} & Ye Liu¹Received
30 January 2013Accepted
4 September 2013Published
26 September 2013Correspondence and
requests for materials
should be addressed toY.L. (ye-liu@imre.a-
star.edu.sg)

¹Institute of Materials Research and Engineering, A *STAR (Agency for Science, Technology and Research), 3 Research Link, Singapore 117602, ²Department of Materials Science & Engineering, National University of Singapore, 9 Engineering Drive 1, 117576 Singapore.

Organic photoluminescent materials are important to many applications especially for diagnosis and detection, and most of organic photoluminescent materials contain fluorophores with extended conjugated structures. Recently some of amino-containing polymers without fluorophores with extended conjugated structure are observed to be photoluminescent, and one possible cause of the photoluminescence is oxidation of the amines. Here we show that photoluminescence can be produced by exposing a typical amino-containing polymer, polyethylenimine, to carbon dioxide. We demonstrate that carbamato anion formed via the reaction between the amine and carbon dioxide is a fluorophore; and the loosely-bound protonated water molecule can increase UV absorption but reduce the photoluminescence emission. Also carbamato anion shows solvent- and excitation wavelength-dependent emission of photoluminescence. The photoluminescence profile of carbamato anion was discussed. These results will facilitate the understanding of photoluminescence observed from amino-containing materials and the design of new fluorophores.

Photoluminescent organic compounds such as proteins^{1–4} and dyes^{5–8} have been explored for bioimaging³, detection^{7,8}, display^{9,10} and solar energy production^{11,12}. Photoluminescence is a process of emission of photons occurred when fluorophores of certain compounds return from an excited state to a lower energy state, and most of the fluorophores usually have extended conjugated structures filled with delocalized electrons which absorb and emit photons, such as p-hydroxybenzylidene-imidazolidone units in fluorescent proteins, fluorescein, rhodamine, and vitamin B₂^{13,14}. However, many types of amino-containing polymers, e.g., poly(amido amines)^{15–25}, poly(amino esters)^{26,27}, polyethylenimine (PEI)^{28,29}, polyurea dendrimer³⁰, without extended conjugated structures have been reported to be photoluminescent since amino-containing dendrimers were reported to be able to emit photoluminescence^{19,31}. Some of these amino-containing polymers have been explored for bioimaging^{15,21,25,29,32}.

Regarding the photoluminescence mechanisms of these amino-containing polymers, one explanation is that oxidation of amines by oxygen in air contributes to the photoluminescence^{16,20}. Considering the feasible reactions between amines and CO₂^{33–36}, it is natural to inquire whether the reaction between the amines and CO₂ from air contributes to photoluminescence observed from amine-containing polymers. Therefore we were motivated to investigate the photoluminescence behavior of amino-containing polymers in the presence of CO₂. Here we show that introduction of CO₂ into a solution of a typical amino-containing polymer, polyethylenimine (PEI) as described in Figure 1, can produce photoluminescence and demonstrate that carbamato anion formed via the reaction between the amine and CO₂ is the fluorophore of the photoluminescence observed. Further the photoluminescence profile of carbamato anion is investigated.

Results

PEI, one of the polymers with the highest amine content, was chosen as a typical amino-containing polymer for the investigation. A suitable UV absorption spectrum could be observed from aqueous solution of PEI containing 50 mM ethylenimine (EI) unit after CO₂ bubbling. UV-Vis absorption and photoluminescence of the solution were measured after bubbling CO₂ at a flow rate of ~ 3 ml/min for 3 h followed by being kept under ambient condition for a certain time. Figure 2A(a) shows the typical UV absorption spectrum and photoluminescence



observed from water solution bubbled with CO_2 , and an aqueous solution of PEI containing 50 mM EI unit after bubbling with N_2 to removing O_2 or at pH 7.0 close to pH value after CO_2 bubbling. Therefore the strong UV absorption and photoluminescence are caused by introducing CO_2 into the aqueous solution of PEI.

As described in Figure 1, the reaction between amine and CO_2 forms carbamate anion via intermediates possibly composed of the loosely-bound encounter complex and zwitterions^{37–39}. Here ^{13}C NMR was applied to monitor the formation of carbamate in a solution of PEI in D_2O bubbled with CO_2 . Figure 2B(b) is ^{13}C NMR spectrum of a solution of PEI in D_2O containing 50 mM EI unit being kept for 5 days after CO_2 bubbling. The peak at 125 ppm is attributed to the dissolved CO_2 , the only peak observed in ^{13}C NMR spectrum of D_2O bubbled with CO_2 as shown in Figure 2B(a). The peak attributed to the carbamate anion appears at 160 ppm^{7,33,40}, and the molar ratio of carbamate anion to the EI unit is determined to be ca. 7.1 : 100 (see supplementary information). In a contrast experiment, $\text{Ba}(\text{OH})_2$ was added to check whether HCO_3^{-1} was formed based on that BaCO_3 is insoluble and barium carbamate is soluble³⁶. The addition of $\text{Ba}(\text{OH})_2$ showed almost no effect on ^{13}C NMR spectrum, so the amount of HCO_3^{-1} formed is negligible. This is reasonable because the kinetic reaction constant of carbamate formation is five orders of magnitude higher than that of HCO_3^{-1} formation^{34,37,38}. There are three types of amine in PEI, i.e., primary amine, secondary amine and tertiary amine with a molar ratio of ca. 1 : 2 : 1 determined from ^{13}C NMR spectrum (see supplementary information). On the basis of the previous work, the reactivity sequence of three types of amine should be primary amine > secondary amine > tertiary amine⁴¹. Therefore the carbamate was formed via the reaction between the primary amines of PEI and CO_2 as described in Figure 1. Bubbling CO_2 into water produced no UV absorption and photoluminescence, hence the carbamate formed is the fluorophore of the photoluminescence observed.

As shown in Figure 2C, both UV absorption peak intensity and photoluminescence intensity from the aqueous solution of PEI bubbled with CO_2 change with the keeping time after CO_2 bubbling. The peak intensity of UV absorption at 364 nm increases with the keeping time before reaching the maximum after being kept for 15 days and then decrease during the observation up to 90 days. Similarly the photoluminescence intensity at 470 nm increases before reaching the maximum after being kept for 21 days and then decreases. Meanwhile Figure 2D shows the effect of the keeping time on the concentration of the carbamate anion and the dissolved CO_2 which were determined from ^{13}C NMR spectra (see supplementary information). The concentration of carbamate anion reaches the maximum after being kept for 21 days and then decreases. When the concentration of carbamate anion reaches the maximum, the molar ratio of carbamate anion to the EI unit is 23 : 100, so the carbamate anion is still formed via the reaction between the primary amine of PEI and the dissolved CO_2 . Meanwhile the concentration of dissolved CO_2 decreases continuously after CO_2 bubbling until being undetectable at 21 days. The consistent reducing concentration of the dissolved CO_2 should be due to the reaction with amine and evaporation into the environment. When the dissolved CO_2 concentration decreases to a certain level, the amount of carbamate starts to decrease due to decarboxylation. Figures 2C and 2D show that there is a coherent relationship between the photoluminescence intensity and the concentration of carbamate anion which further confirms that carbamate anion is the fluorophore of the photoluminescence observed.

Also Figure 2C reflects that there is a discrepancy between the effect of keeping time on the UV absorption intensity and the photoluminescence intensity. While the maximum of UV absorption is obtained after being kept for 15 days, the photoluminescence intensity reaches the highest value at 21 days. These indicate that there are more than one type of fluorophore contributing to UV absorbance

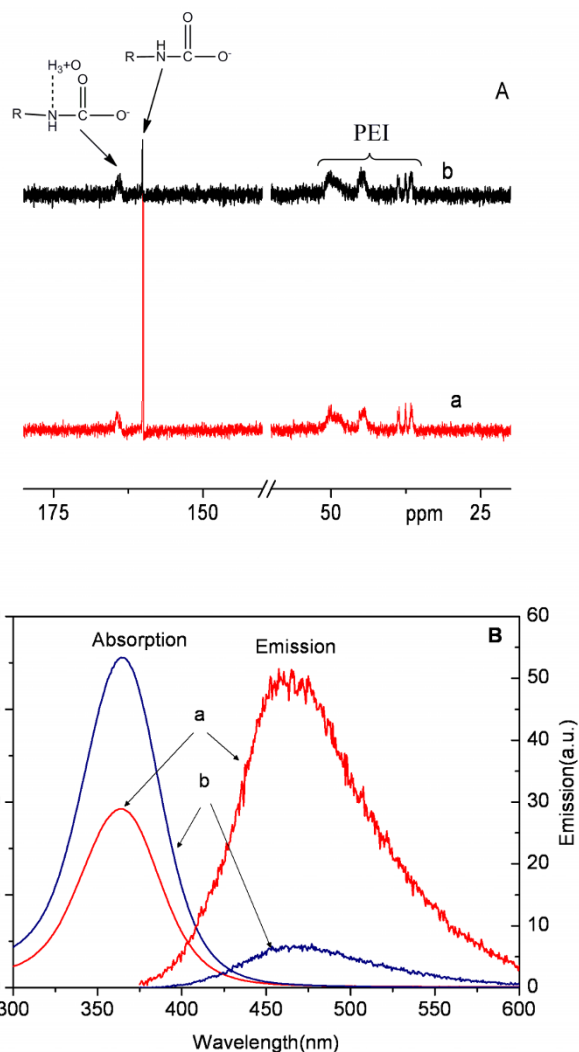


Figure 3 | (A) ^{13}C NMR spectra of a solution of PEI in D_2O containing 4.6 M EI unit being kept for 15 days after CO_2 bubbling (a) before and (b) after thermal treatment at 60°C for 3 h under N_2 . (B) UV-Vis absorption and photoluminescence spectra with excitation at 364 nm of an aqueous solution of PEI containing 50 mM EI unit being kept for 15 days after CO_2 bubbling (a) before and (b) after thermal treatment at 60°C for 3 h under N_2 .

and photoluminescence; otherwise a unanimous variation tendency should be observed. The other types of fluorophore should be the intermediates of carbamate anion formed when the dissolved CO_2 was still presented. However no corresponding peaks can be observed in Figure 2B(b) even though the ^{13}C NMR spectrum was collected for 3 days due to a high ratio of noise to signal caused by the low concentration of PEI. In order to reduce the ratio of noise to signal, the concentration of PEI was increased by around 100 times to containing 4.6 M EI unit. Figure 3A(a) shows the ^{13}C NMR spectrum of the solution of PEI in D_2O containing 4.6 M EI unit being kept for 15 days after CO_2 bubbling (also formation of HCO_3^{-} under this condition is negligible indicated by the insignificant effect of adding $\text{Ba}(\text{OH})_2$ on the ^{13}C NMR spectrum.). In comparison with Figure 2B(b), a new broad peak appears at 164 ppm. This peak is ascribed to the loosely-bound encounter complex rather than zwitterions because the down-field shifting of the peaks attributed to carbon in the zwitterions should be more due to the positively charged nitrogen. The loosely-bound encounter complex with a different bound degree results in the broad peak in the ^{13}C NMR

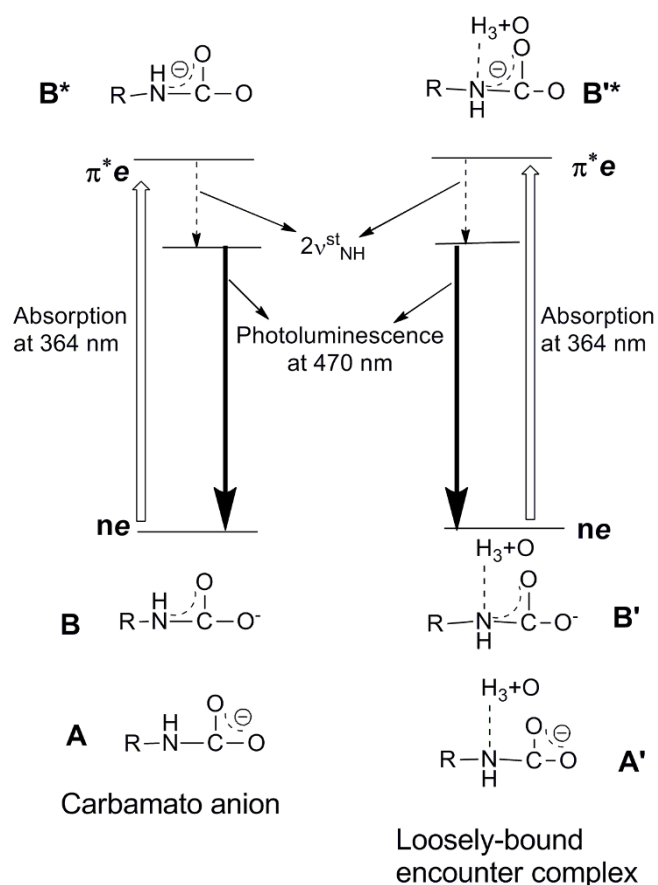


Figure 4 | Photoluminescence profile of carbamate anion.

spectrum. Therefore, the loosely-bound encounter complex is the dominant intermediate of carbamate anion as reported³⁹. Hence both carbamate anion and the loosely-bound encounter complex contribute to the photoluminescence observed.

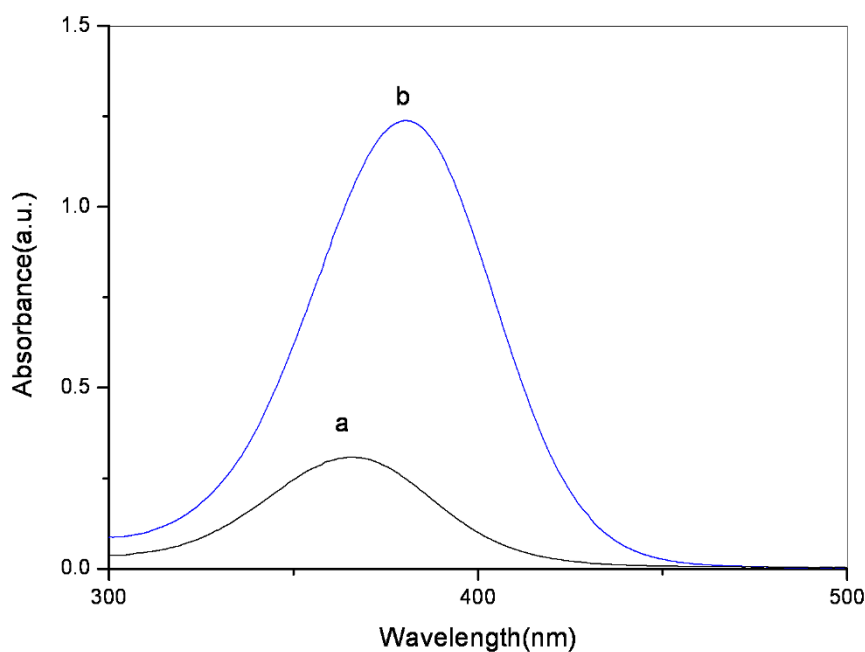


Figure 5 | UV-Vis absorption of a solution of PEI containing 50 mM EI unit being kept for 5 days after CO_2 bubbling in (a) water and (b) methanol.

We found that thermal treatment could change the equilibrium between carbamate anion and the loosely-bound encounter complex; therefore thermal treatment was applied to differentiate the photoluminescent behaviors of carbamate anion and the loosely-bound encounter complex. Figure 3A shows ^{13}C NMR spectrum of the solution of PEI in D_2O containing 4.6 M EI unit being kept for 15 days after CO_2 bubbling before and after thermal treatment at 60°C for 3 h under N_2 . The molar ratio of the loosely-bound encounter complex to carbamate anion is shown to increase from 1.76 to 1.94 with the molar ratio of the total carbamate to the EI unit being kept at ca. 35 : 100 (see supplementary information). So the thermal treatment shifts the equilibrium towards the formation of the loosely-bound encounter complex (the degradation of carbamate to recover amines and remove CO_2 occurs at 100°C above³³). Accordingly, the effects of thermal treatment at 60°C for 3 h under N_2 on the UV absorption and photoluminescence of aqueous solution of PEI containing 50 mM EI unit being kept for 15 days after CO_2 bubbling was investigated. As shown in Figure 3B, the thermal treatment reduces photoluminescence intensity at 470 nm from 1.75 a.u. to 0.17 a.u. but increases the UV absorption at 364 nm from 0.8 a.u. to 1.8 a.u. Hence the loosely binding of H_3O^+ to carbamate anion results in a higher UV absorption but a lower photoluminescence emission.

Discussion

As shown in Figure 4, there are two 3-atoms (either N, C and O or 2 O and C) containing resonance structures, i.e., A and B, for carbamate anion, without instable π -conjugated 4-atoms containing (N, C and 2 O) resonance structures with one anti-bonding orbital being filled with electrons^{42–47}. Accordingly, there are two resonance structures for the loosely-bound encounter complex, i.e., A' and B'. Among these resonance structures, A and A' are the major components because O atom is more electronegative than N atom. However, $n \rightarrow \pi^*$ transition should only occur in B and B' with n electron from the negatively charged O atom jumping to the conjugated unit composed of N, C and O atoms, but is prohibited in A and A' due to electronic repulsion between n electron of N atom and electrons on the carboxylate ion. Hence B and B' are the dominant fluorophores. The $n \rightarrow \pi^*$ transition of B and B' under UV irradiation is supported by the red-shift in UV absorption from 364 nm

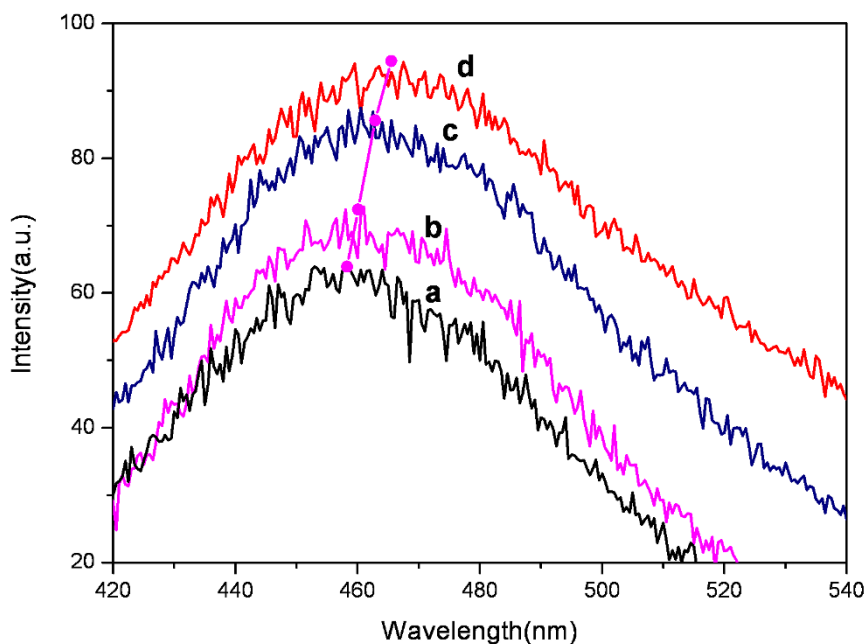


Figure 6 | Photoluminescence emission spectra of an aqueous solution of PEI containing 50 mM EI unit being kept for 10 days after CO₂ bubbling being excited at (a) 330 nm; (b) 340 nm; (c) 350 nm; and (d) 360 nm.

to 380 nm when water is substituted by methanol as shown in Figure 5, because $n \rightarrow \pi^*$ transition shows a red-shift and $\pi \rightarrow \pi^*$ transition shows a blue-shift reversely when solvent molecules have lower polarity and form hydrogen bonding with a lower strength¹⁴, and methanol has a lower polarity and forms a weaker hydrogen bonding with carbamate than water^{48,49}. In comparison with B, the loosely-bound H₃⁺O in B' facilitates the $n \rightarrow \pi^*$ transition of electron, and the H₃⁺O in the excited state B'* reduces the feasibility of relaxation of the excited electrons. These should be the cause of the stronger UV absorption but a weaker photoluminescence emission observed for carbamate anion loosely bonded with H₃⁺O.

As shown in Figure 2A, the frequency difference between the excitation at 364 nm (wavenumber: 27472 cm⁻¹) and the emission at 470 nm (wavenumber: 21276 cm⁻¹) is 6196 cm⁻¹. This difference is ca. two times of the stretching vibration frequency of N-H ($\nu_{\text{NH}}^{\text{st}}$) or O-H ($\nu_{\text{OH}}^{\text{st}}$) which are ca. 3300 cm⁻¹ as reflected in FTIR spectrum of aqueous solution of PEI (see supplementary information Fig. S4). When H₂O is substituted by D₂O, Figure 2A(d) shows that the emission peaks shift to 442 nm (wavenumber: 22624 cm⁻¹), with the emission peak being kept at 364 nm. The frequency difference between excitation at 364 nm (wavenumber: 27472 cm⁻¹) and the emission peaks are 4848 cm⁻¹ which are close to two time of the vibration frequency of N-D ($\nu_{\text{ND}}^{\text{st}}$) or O-D ($\nu_{\text{OD}}^{\text{st}}$) of ca. 2400 cm⁻¹ as shown in FTIR (see supplementary information Fig. S4). Further, Figure 6 shows a typical excitation wavelength-depend photoluminescence profile, which was obtained from an aqueous solution of PEI containing 50 mM EI unit being kept for 10 days after CO₂ bubbling. The photoluminescence emission wavelength depends on the excitation wavelength with the frequency difference between the excitation and the emission being almost kept constant to be two times of $\nu_{\text{NH}}^{\text{st}}$ or $\nu_{\text{OH}}^{\text{st}}$. So one important nonradiative process of the excited B* and B'* is via stretching vibration of N-H or O-H⁵⁰, and preferably via the intramolecular N-H of carbamate anion in comparison with the O-H of water^{13,14}.

In order to understand the functions of polymer morphology in the photoluminescence observed, butylamine was adopt to substitute PEI, and the solution of butylamine in methanol was prepared. No UV absorption could be observed from a solution of 50 mM butylamine in methanol being kept for 5 days after CO₂ bubbling (see

supplementary information Fig. S5). However, carbamate was formed as reflected in ¹³C NMR spectrum of a solution of 4.6 M butylamine in methanol being kept for 5 days after CO₂ bubbling (see supplementary information Fig. S6). So fluorescence quenching of small carbamate easily occurs, and polymer morphology is important in avoiding the fluorescence quenching of all the conjugated carbamate.

Photoluminescence can be produced by exposing aqueous solution of PEI to CO₂. Carbamate anion formed via the reaction between the amines of PEI and CO₂ contribute to the photoluminescence. The loosely binding of H₃⁺O to carbamate anion results in a higher UV absorption and a lower photoluminescence emission, probably due to a facilitated $n \rightarrow \pi^*$ transition and a retarded relaxation of the excited electron. The photoluminescence emission wavelength of carbamate anion depends on the solvent type and the excitation wavelength, and the nonradiative process is via stretching vibration of the N-H in the carbamate anion. Considering the common existence of CO₂, the reaction with CO₂ should be one of the causes of photoluminescence observed from amino-containing polymers.

Methods

Materials. Hyperbranched Poly(ethyleneimine) (PEI) (M_n : 600), butylamine, barium hydroxide, methanol, and deuterium oxide (D₂O) were purchased from Aldrich and used as received.

Characterization techniques. ¹³C NMR spectra were recorded on a Bruker ACF 400 FT-NMR spectrometer. The absorption and photoluminescence spectrum measurements were conducted on a Shimadzu UV-1601 PC UV-Vis spectrophotometer and a Perkin-Elmer Instrument LS 55 luminescence spectrometer, respectively. In order to get comparable photoluminescence intensity, all experimental parameters were kept fixed for all emission scans. FT-IR spectra of PEI solution on CaF₂ plate were collected in a frequency range of 1000–4000 cm⁻¹ with 2 cm⁻¹ resolution and 64 scans on a FTIR spectrometer Spectrum 2000 (Perkin Elmer) in a transmission mode.

Exposed PEI to CO₂. For UV-Vis absorbance and photoluminescence scans, CO₂ was introduced to a solution of PEI containing 50 mM EI in 10 ml of water or methanol in a 20 ml vial at a flow rate of ~ 3 ml/min for 3 h using a one needle-inlet and one needle-outlet configuration. Then the solution was kept for a designed time before measurements. For ¹³C NMR experiments, D₂O was used instead and the concentration of EI unit was 50 mM and 4.6 M, respectively.



Thermal treatment procedure. Aqueous solution of PEI containing 50 mM EI being kept for 15 days after CO₂ bubbling was put into an oil bath at 60 °C under nitrogen for 3 hours before UV-Vis absorbance and photoluminescence scan were conducted. For ¹³C NMR experiment, a solution of PEI in D₂O containing 4.6 M EI unit was heated at 60 °C for 3 hours under nitrogen just before NMR experiment. All UV-Vis absorbance measurement, photoluminescence scan and NMR experiments were finished in less than 5 minutes.

- Shaner, N. C., Steinbach, P. A. & Tsien, R. Y. A guide to choosing fluorescent proteins. *Nat. Methods* **2**, 905–909 (2005).
- Tsien, R. Y. The green fluorescent protein. *Annu. Rev. Biochem.* **67**, 509–544 (1998).
- Lippincott-Schwartz, J. & Patterson, G. H. Development and use of fluorescent protein markers in living cells. *Science* **300**, 87–91 (2003).
- Zhang, J., Campbell, R. E., Ting, A. Y. & Tsien, R. Y. Creating new fluorescent probes for cell biology. *Nat. Rev. Mol. Cell Biol.* **3**, 906–918 (2002).
- Tavasli, M. et al. Colour tuning from green to red by substituent effects in phosphorescent tris-cyclometalated iridium(III) complexes of carbazole-based ligands: synthetic, photophysical, computational and high efficiency OLED studies. *J. Mater. Chem.* **22**, 6419–6428 (2012).
- Kim, M. J. et al. Tuning of spacer groups in organic dyes for efficient inhibition of charge recombination in dye-sensitized solar cells. *Dyes Pigm.* **95**, 134–141 (2012).
- Liu, Y. et al. Fluorescent Chemosensor for Detection and Quantitation of Carbon Dioxide Gas. *J. Am. Chem. Soc.* **132**, 13951–13953 (2010).
- Liu, Y. et al. Specific Detection of D-Glucose by a Tetraphenylethene-Based Fluorescent Sensor. *J. Am. Chem. Soc.* **133**, 660–663 (2011).
- Singh, R., Unni, K. N. N., Solanki, A. & Deepak. Improving the contrast ratio of OLED displays: An analysis of various techniques. *Opt. Mat.* **34**, 716–723 (2012).
- Wang, C. S., Nishida, J., Bryce, M. R. & Yamashita, Y. Synthesis, Characterization, and OFET and OLED Properties of pi-Extended Ladder-Type Heteroacenes Based on Indolodibenzothiophene. *Bull. Chem. Soc. Jpn.* **85**, 136–143 (2012).
- Oregan, B. & Gratzel, M. A Low-Cost, High-Efficiency Solar-Cell Based on Dye-Sensitized Colloidal TiO₂ Films. *Nature* **353**, 737–740 (1991).
- Yella, A. et al. Porphyrin-Sensitized Solar Cells with Cobalt (II/III)-Based Redox Electrolyte Exceed 12 Percent Efficiency. *Science* **334**, 629–634 (2011).
- Itoh, T. Fluorescence and Phosphorescence from Higher Excited States of Organic Molecules. *Chem. Rev.* **112**, 4541–4568 (2012).
- Bernard, Valeur. *Molecular Fluorescence: Principles and Applications* (Wiley-VCH Verlag GmbH, Weinheim (Federal Republic of Germany), 2001).
- Chen, Y. et al. Photoluminescent Hyperbranched Poly(amido amine) Containing beta-Cyclodextrin as a Nonviral Gene Delivery Vector. *Bioconjugate Chem.* **22**, 1162–1170 (2011).
- Chu, C. C. & Imae, T. Fluorescence Investigations of Oxygen-Doped Simple Amine Compared with Fluorescent PAMAM Dendrimer. *Macromol. Rapid Commun.* **30**, 89–93 (2009).
- Jasmine, M. J. & Prasad, E. Fractal Growth of PAMAM Dendrimer Aggregates and Its Impact on the Intrinsic Emission Properties. *J. Phys. Chem. B* **114**, 7735–7742 (2010).
- Jiang, G. H., Wang, Y., Sun, X. K. & Shen, J. J. Facile one-pot approach for preparing fluorescent and biodegradable hyperbranched poly(amidoamine)s. *Polym. Chem.* **1**, 618–620 (2010).
- Lee, W. I., Bae, Y. J. & Bard, A. J. Strong blue photoluminescence and ECL from OH-terminated PAMAM dendrimers in the absence of gold nanoparticles. *J. Am. Chem. Soc.* **126**, 8358–8359 (2004).
- Lin, S. Y. et al. Unraveling the Photoluminescence Puzzle of PAMAM Dendrimers. *Chem. Eur. J.* **17**, 7158–7161 (2011).
- Tsai, Y. J., Hu, C. C., Chu, C. C. & Toyoko, I. Intrinsically Fluorescent PAMAM Dendrimer as Gene Carrier and Nanoprobe for Nucleic Acids Delivery: Bioimaging and Transfection Study. *Biomacromolecules* **12**, 4283–4290 (2011).
- Wang, D., Imae, T. & Miki, M. Fluorescence emission from PAMAM and PPI dendrimers. *J. Colloid Interface Sci.* **306**, 222–227 (2007).
- Yang, W. & Pan, C. Y. Synthesis and Fluorescent Properties of Biodegradable Hyperbranched Poly(amido amine)s. *Macromol. Rapid Commun.* **30**, 2096–2101 (2009).
- Yang, W., Pan, C. Y., Luo, M. D. & Zhang, H. B. Fluorescent Mannose-Functionalized Hyperbranched Poly(amido amine)s: Synthesis and Interaction with E. coli. *Biomacromolecules* **11**, 1840–1846 (2010).
- Yang, W., Pan, C. Y., Liu, X. Q. & Wang, J. Multiple Functional Hyperbranched Poly(amido amine) Nanoparticles: Synthesis and Application in Cell Imaging. *Biomacromolecules* **12**, 1523–1531 (2011).
- Shen, Y. Q. et al. Degradable Dual pH- and Temperature-Responsive Photoluminescent Dendrimers. *Chem. Eur. J.* **17**, 5319–5326 (2011).
- Wu, D. C., Liu, Y., He, C. B. & Goh, S. H. Blue photoluminescence from hyperbranched poly(amino ester)s. *Macromolecules* **38**, 9906–9909 (2005).
- Pastor-Perez, L., Chen, Y., Shen, Z., Lahoz, A. & Stiriba, S. E. Unprecedented blue intrinsic photoluminescence from hyperbranched and linear polyethylenimines: Polymer architectures and pH-effects. *Macromol. Rapid Commun.* **28**, 1404–1409 (2007).
- Lin, S. Y. et al. One-pot synthesis of linear-like and photoluminescent polyethylenimines for intracellular imaging and siRNA delivery. *Chem. Commun.* **46**, 5554–5556 (2010).
- Restani, R. B. et al. Biocompatible Polyurea Dendrimers with pH-Dependent Fluorescence. *Angew. Chem. Int. Ed.* **51**, 5162–5165 (2012).
- Wang, D. J. & Imae, T. Fluorescence emission from dendrimers and its pH dependence. *J. Am. Chem. Soc.* **126**, 13204–13205 (2004).
- Restani, R. B. et al. Biocompatible Polyurea Dendrimers with pH-Dependent Fluorescence. *Angew. Chem. Int. Ed.* **51**, 5162–5165 (2012).
- Sayari, A., Heydari-Gorji, A. & Yang, Y. CO₂-Induced Degradation of Amine-Containing Adsorbents: Reaction Products and Pathways. *J. Am. Chem. Soc.* **134**, 13834–13842 (2012).
- Hampe, E. M. & Rudkevich, D. M. Reversible covalent chemistry of CO₂. *Chem. Commun.* 1450–1451 (2002).
- Hampe, E. M. & Rudkevich, D. M. Exploring reversible reactions between CO₂ and amines. *Tetrahedron* **59**, 9619–9625 (2003).
- Dell'Amico, D. B., Calderazzo, F., Labella, L., Marchetti, F. & Pampaloni, G. Converting carbon dioxide into carbamate derivatives. *Chem. Rev.* **103**, 3857–3897 (2003).
- Caplow, M. Kinetics of Carbamate Formation and Breakdown. *J. Am. Chem. Soc.* **90**, 6795–6803 (1968).
- Crooks, J. E. & Donnellan, J. P. Kinetics of the Formation of N,N-Dialkylcarbamate from Diethanolamine and Carbon-Dioxide in Anhydrous Ethanol. *J. Chem. Soc., Perkin Trans.* **2** 191–194 (1988).
- Crooks, J. E. & Donnellan, J. P. Kinetics and Mechanism of the Reaction Between Carbon-Dioxide and Amines in Aqueous-Solution. *J. Chem. Soc., Perkin Trans.* **2** 331–333 (1989).
- Kim, Y. E., Choi, J. H., Nam, S. C. & Yoon, Y. I. CO₂ Absorption Characteristics in Aqueous K₂CO₃/Piperazine Solution by NMR Spectroscopy. *Ind. Eng. Chem. Res.* **50**, 9306–9313 (2011).
- Wu, D. C., Liu, Y., He, C. B., Chung, T. S. & Goh, S. T. Effects of chemistries of trifunctional amines on mechanisms of Michael addition polymerizations with diacrylates. *Macromolecules* **37**, 6763–6770 (2004).
- Olah, G. A. & Calin, M. Stable Carbonium Ions. 59. Protonated Alkyl Carbamates and Their Cleavage to Protonated Carbamic Acids and Alkylcarbonium Ions. *J. Am. Chem. Soc.* **90**, 401–& (1968).
- Olah, G. A. & White, A. M. Stable Carbonium Ions. 64. Protonated Carbonic Acid (Trihydroxycarbonium Ion) and Protonated Alkyl (Aryl) Carbonates and Hydrogen Carbonates and Their Cleavage to Protonated Carbonic Acid and Carbonium Ions Possible Role of Protonated Carbonic Acid in Biological Carboxylation Processes. *J. Am. Chem. Soc.* **90**, 1884–& (1968).
- Rogers, M. T. & Woodbrey, J. C. Proton Magnetic Resonance Study of Hindered Internal Rotation in Som Substituted N,N-Dimethylamides. *J. Phys. Chem.* **66**, 540–& (1962).
- Pitner, T. P., Sternglanz, H., Bugg, C. E. & Glickson, J. D. Proton Nuclear Magnetic-Resonance Study of Hindered Internal-Rotation of Dimethylamino Group of N₆,N₆-Dimethyladenine Hydrochloride in Aqueous-Solution. *J. Am. Chem. Soc.* **97**, 885–888 (1975).
- Lustig, E., Benson, W. R. & Duy, N. Hindered Rotation in N,N-Dimethylcarbamates. *J. Org. Chem.* **32**, 851–& (1967).
- White, E. H., Chen, M. C. & Dolak, L. A. N-Nitroamides and N-Nitrocarbamates. 3. Rotational Isomerism Steric Effects and Physical Properties at Low Temperatures. *J. Org. Chem.* **31**, 3038–& (1966).
- Reichardt, C. & Welton, T. *Solvents and Solvent Effects in Organic Chemistry* (Wiley-VCH Publishers, 2010).
- Hansen, C. M. *Hansen Solubility Parameters: A User's Handbook* (CRC PressINC, 2007).
- Petrenko, T., Krylova, O., Neese, F. & Sokolowski, M. Optical absorption and emission properties of rubrene: insight from a combined experimental and theoretical study. *New J. Phys.* **11** (2009).

Acknowledgments

We appreciate the finance support from A*Star.

Author contributions

X.Y.P. and Y.L. contributed the experiments design and the results analysis, wrote and reviewed the manuscript. G.W. contributed the experiments and manuscript writing. C.L.L., B.H.T. and C.B.H. contributed to the results analysis.

Additional information

Supplementary information accompanies this paper at <http://www.nature.com/scientificreports>

Competing financial interests: The authors declare no competing financial interests.

How to cite this article: Pan, X. et al. Photoluminescence from Amino-Containing Polymer in the Presence of CO₂: Carbamate Anion Formed as a Fluorophore. *Sci. Rep.* **3**, 2763; DOI:10.1038/srep02763 (2013).



This work is licensed under a Creative Commons Attribution-NonCommercial-ShareAlike 3.0 Unported license. To view a copy of this license, visit <http://creativecommons.org/licenses/by-nc-sa/3.0>